ADVANCED ENGINEERING MATERIALS
www.aem-journal.com

Temperature Effect on Performance of Triboelectric Nanogenerator

*Cun Xin Lu, Chang Bao Han, Guang Qin Gu, Jian Chen, Zhi Wei Yang, Tao Jiang, Chuan He, and Zhong Lin Wang**

The triboelectric nanogenerator (TENG) is a promising energy harvesting technology that can convert mechanical energy into electricity and can be used as self-powered active sensors. However, previous studies are mostly carried out at room temperature without considering the temperature effect on the electrical performance of TENGs, which is critical for the application of electronics powered by TENGs in different regions in the world. In the present work, a TENG that worked in the single-electrode and contact-separation mode is utilized to reveal the influence of environment temperature on the electrical performance of TENG. The electrical performance of the TENG shows a decreasing tendency, as the temperature rises from −20 to 150 °C, which is controlled by the temperature-induced changes in the ability of storing and gaining electrons for polytetrafluoroethylene (PTFE). The storing electron ability change of PTFE is attributed to two aspects: one is the reduction of relative permittivity of PTFE sheet as the temperature increases, and the other is the variations of effective defects such as the escape of trapped charges in shallow traps and surface oxidation under the effect of temperature perturbation. This work can provide useful information for the application of TENG in both electric power generation and self-powered sensors in the harsh environment.

1. Introduction

With the growing threat of limited fossil fuels and related environmental issues, searching for renewable energy sources from ambient environment becomes necessary for the sustainable development of human civilization. Harvesting neglected energy of the ambient environment to power electronic devices[1–4] is a good choice to solve the energy crisis. Nowadays, a notable technological trend is the rapid growth of self-powered electronics for applications in communication, personal health care, and environmental monitoring, especially applying in harsh environments, such as under high/low temperature,[5,6] high humidity,[7,8] or corrosive conditions.[9,10] In recent years, many studies have proved that the TENG is a simple and attractive approach for converting ambient mechanical energy into electricity,[11–14] which can be used as a potentially competitive power source for self-powered electronic devices.[15–18] It is very important and interesting to explore the effect of temperature on the electrical performance of TENG, especially when the self-powered electronics powered by TENG are used in some extreme conditions such as the frigid zones, and desert regions. However, there are few studies about this temperature effect on the output performance of TENG. Although several publications showed that the dependence of electrical output of TENG at different temperature conditions,[19,20] the principle how the temperature affects the electrical performance of the TENG is still not clear.

Here, a TENG which worked in single-electrode mode was used to reveal the output characteristics of TENG in various temperature environments. Its short-circuit current and output power ranges from 1.45 to 0.875 μA and from 0.3943 to 0.1157 $W m^{-2}$, respectively, under a low working frequency of 3 Hz when the temperature varies from −20 to 150 °C. The affecting principle of the temperature on the electrical outputs was investigated by measuring the relative permittivity of PTFE sheet, the theoretical calculations, and the characterizations of PTFE surface. The results proved that the output performance of TENG at different temperature conditions is associated with the gaining/storing electron ability of PTFE sheet. This work will provide a reference for the application of wearable electronics in harsh environments.

2. Experimental Section

Fabrication of the TENG: The TENG in this work was made up of a Al foil (55 × 55 × 1 mm), polyethylene terephthalate (PET) insulation tapes, PTFE sheets (55 × 55 × 3 mm). The PTFE sheet is a commercial product

Prof. Z. L. Wang
School of Materials Science and Engineering,
Georgia Institute of Technology,, Atlanta, Georgia
30332-0245, USA
E-mail: zhong.wang@mse.gatech.edu

C. X. Lu, Dr. C. B. Han, G. Q. Gu,
J. Chen, Z. W. Yang, Dr. T. Jiang,
Dr. C. He, Prof. Z. L. Wang
Beijing Institute of Nanoenergy and
Nanosystems, Chinese Academy of Sciences,
Beijing, 100083, China

The ORCID identification number(s) for the author(s) of this article can be found under https://doi.org/10.1002/adem.201700275.

Cun Xin Lu and Chang Bao Han contribute equally to this work.

DOI: 10.1002/adem.201700275

that was purchased from DuPont Company. It was used as one of two friction layers for its outstanding electronegativity,[21] low frictional coefficient,[22,23] and high thermostability.[24] The Al foil that has excellent electrical conductivity serves as an electrode and another friction layer. As shown in **Figure 1**a, the PTFE sheet and Al foil were fixed on two supporting plates with the help of PET insulation tape. The component of PTFE and its supporting plate attached to a push rod of linear vibration generator serves as the movable part. The linear vibration generator with tunable frequency and amplitude acted as the vibration source that provides the mechanical vibration for the TENG.

Electrical Measurement of the TENG: To investigate the electrical output performance of TENG devices in various temperatures, the whole device was placed in a high-low temperature-testing chamber (Wuxi ZhongTian, GDW-50L). To keep the testing temperature stable, an interval of 10 min was reserved to re-establish the thermal equilibrium in the chamber during the test process. Five hundred and forty cycles were performed at each test to ensure the stability of electric output. The output frequency of vibration source was set to be 3 Hz. Throughout the testing process, the relative humidity in chamber was controlled within $10 \pm 2\%$. The short-circuit current, open-circuit voltage, and transferred charge were measured by the current amplifier (Keithley 6514, USA), oscilloscope (Agilent DSO-X 2014A, USA) and low-noise preamplifier (Keithley SR570, USA), respectively.

Relative Permittivity Test: The relative permittivity of the PTFE sheet was tested through a LCR meter (4263B, Agilent, USA) in a variable temperature system. Firstly, the PTFE sheet was inserted between two Parallel plate electrodes to form a plate capacitor. Then, the capacitances were tested under a frequency of 100 KHz. Finally, the relative permittivity of PTFE sheets was obtained by the parallel-plate capacitor formula.

Characterization of the PTFE Sheets: The physical, chemical, and structural properties of the PTFE surface were studied by the means of IR, SEM, and XPS.

Finite Element Method Simulations: In the finite element method (FEM) simulations, we used the "electrostatics" module of COMSOL to calculate the electric potential distribution through the "stationary" study. First, we constructed the model of TENG used for simulation in this work. The geometry parameters of the parts of model are as follows: the length and width of both friction materials are 55 and 55 mm, respectively; the thickness of aluminum foil and PTFE sheet, respectively, are 0.4 and 3 mm. The gap between aluminum foil and PTFE is 10 mm. Second, in the "material" section, we selected the aluminum and PTFE materials. The relative permittivity of PTFE was set to be 2.0. Third, the boundary conditions such as the surface charge density was be set and the mesh was built on the model by subdivision triangular grid. Finally, we could implement the computation to obtain the electric potential information.

3. Result and Discussion

3.1. Working Principle of the TENG

The working principle of TENG in one cycle has been schematically depicted in Figure 1b–e. In this paper, the term surface is referred to a thin surface layer that thickness is small, compared to the PTFE sheet thickness. Owing to the fact that two contacting materials have different abilities to attract electrons,[25] the surface charge transfer will take place on the contact interface between Al electrode and PTFE during a contact process. More specifically, the PTFE has higher electron affinity and higher work function than aluminum,[26,27] negative triboelectric charges would be injected from Al to PTFE sheet, and equal positive charges will be left on Al electrode during the contact process shown in Figure 1b. Other works have revealed that dielectric materials such as PTFE could keep charges for a long time.[25,28,29] The negative charges on the PTFE sheet could induce positive charges on the Al electrode. The positive inductive charges on the Al electrode will be reduced when the PTFE sheet move upwards to add the distance between two materials, as shown in Figure 1c. The decrease in positive induced charges on the Al electrode can be understood as a consequence of being counteracted by same amount of electrons that flow from ground to Al electrode through external circuit. Figure 1d describes the inductive charges on the Al electrode is reduced further as the distance between two materials continues to augment. On the contrary,

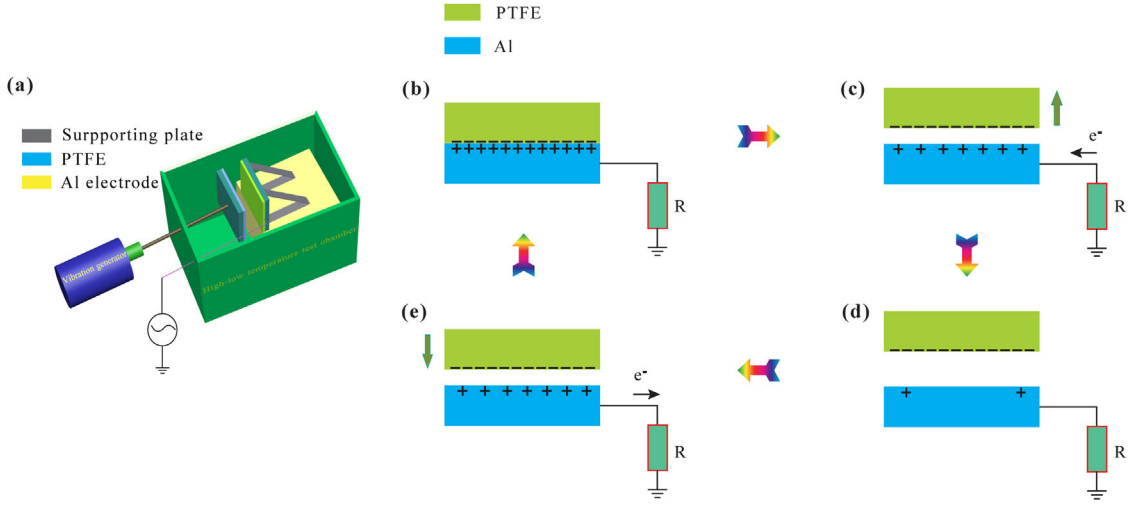

Figure 1. a) Schematic diagram of experimental set-up. b–e) The working principle of the TENG during one cycle: b) The PTFE sheet contacted with the Al electrode. c) The PTFE sheet move upwards to add the distance between two materials, and the positive inductive charges on the Al electrode to be reduced, causing the negative charges to flow from the ground to the Al electrode. d) The PTFE sheet continues to move upwards further until the positive inductive charges on Al electrode decreased to minimum value. There is no charges to flow. e) The PTFE sheet move downwards to reduce the distance between two materials, causing negative charges to flow from the Al electrode to the ground.

the inductive charges on the Al electrode is increased as the PTFE sheet move downwards to diminish the distance between two materials, as shown in Figure 1e. The electrons will flow from Al electrode to ground through external circuit. Therefore, the output current, whose direction relies on the mechanical motion direction, can be formed by the flow of induced charges on the Al electrode.

3.2. The Electrical Performance of TENG Under Virous Temperature Conditions

Figure 2 illustrates the electrical performance of TENG, including the short-circuit current (I_{sc}), open-circuit voltage (V_{oc}), and short-circuit transferred charges (ΔQ_{sc}). **Figure 3**a–c illustrate the I_{sc}, V_{oc}, and ΔQ_{sc} of TENG signal curves at −20, −10, 0, 20, 60, 100, 130, and 150 °C, respectively. It shows intuitively that the electrical output of TENG could stay stable at each temperature point. Figure 2d–f, respectively, shows that the V_{oc}, I_{sc}, and ΔQ_{sc} decrease with the augment of temperature from −20 to 20 °C. Although the V_{oc} and I_{sc} have a tendency of small increasing when the temperature changes from 20 to 60 °C, they can be regarded as keeping stable in the whole temperature range of 20–100 °C, but drop rapidly when the temperature grows continuously, as shown in Figure 2d and e, respectively. This result is consistent with Wen's study[19]. Figure 2f shows that ΔQ_{sc} increases as the temperature rises from 20 to 60 °C, but decreases rapidly when the temperature is over 100 °C or below 20 °C.

3.3. The FEM Simulation Result and Relative Permittivity of PTFE

The relative permittivity of PTFE sheet is a function of temperature shown in Figure 3a. The measurement of PTFE's relative permittivity is accordant with results of previous researches.[30,31] For a nonpolarity solid dielectric such as PTFE sheet, the variation of relative permittivity will be caused by thermal expansion according to the Clausius–Mossotti relation. The inset of **Figure 4**b shows the schematic diagram of utilizing the TENG to charge a capacitor through a rectifier bridge. The higher the temperature, the lower charging voltage of capacitor becomes within a same charging time, as described in Figure 3b.

Additionally, the space potential distribution between the PTFE and the Al electrode had been simulated when the TENG works at different temperatures of −20, 20, 60, and 150 °C, as shown in Figure 3c–f, respectively. The maximum of electric potential can be reached to 825 V (−20 °C), 700 V (20 °C), 720 V (60 °C), and 400 V (150 °C). It indicates that the temperature may stimulate the surface electric potential to decay. The variation trend of simulation results is similar to the measured result shown in Figure 2d.

As discussed above, the temperature indeed affects the electrical performance of TENG. Two reasons that contribute to this temperature-induced effect are as follows.

3.4. The Theoretical Calculation

Firstly, as we know, the permittivity of a medium describes how much electric field is generated per unit charge in that medium, which also means the ability of storing charges in materials. Therefore, the diminution of relative permittivity will reduce the number of electrons stored on the PTFE surface. There are many previous researches about the contact electrifi cation.[32–35] The volume charge density on the PTFE sheet during the process of metal-insulator

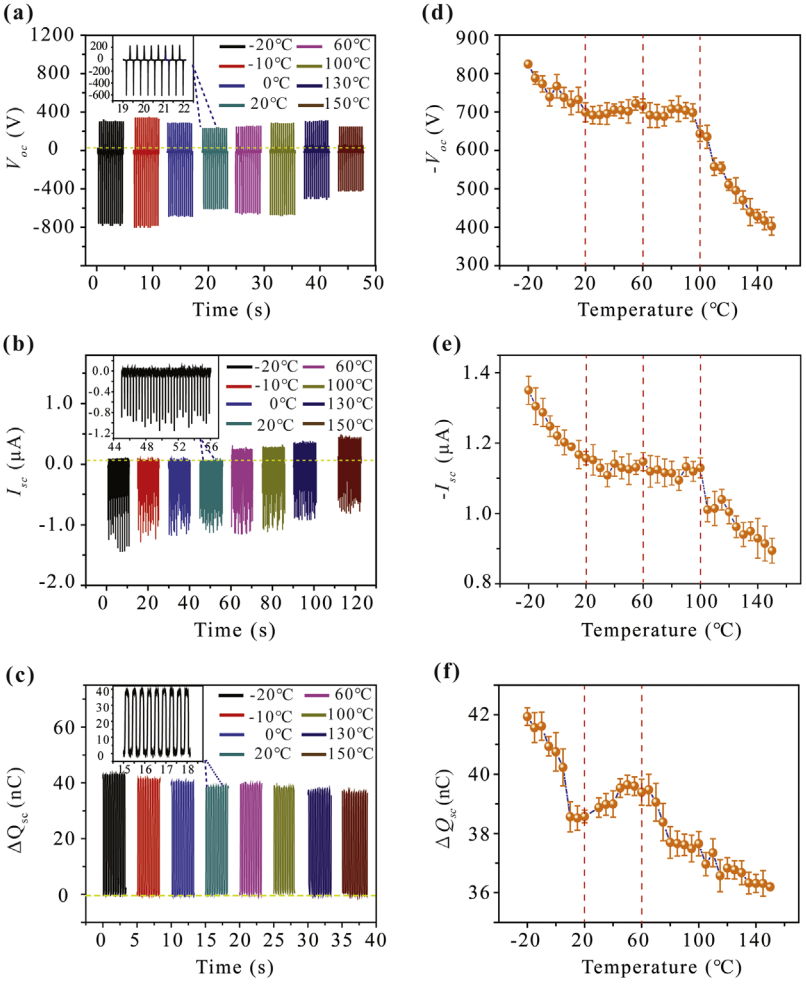

Figure 2. a–c) Show the electrical signal curves of short-circuit current (I_{sc}), open-voltage (V_{oc}), and short-circuit transferred charges (ΔQ_{sc}), respectively, at −20, −10, 0, 20, 60, 100, 130, and 150 °C. The inset in Figure 3a–c shows, respectively, the enlarged view of I_{sc}, V_{oc}, and ΔQ_{sc} at 20 °C. d–f) describe, respectively, I_{sc}, V_{oc}, and ΔQ_{sc} in the temperature range of −20–150 °C.

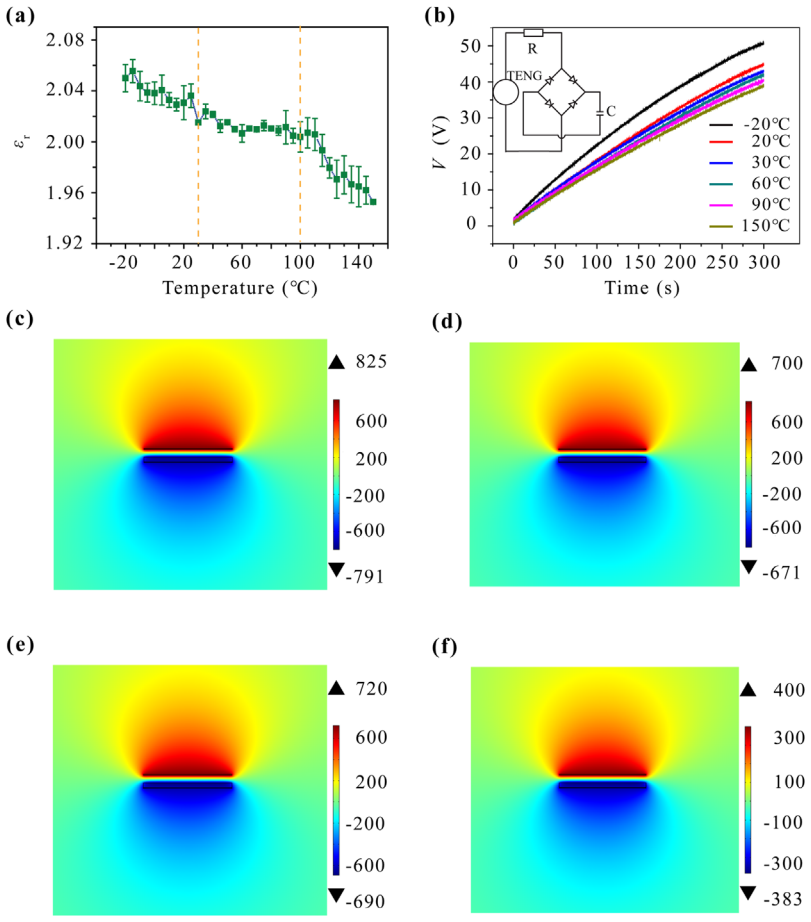

Figure 3. a) Shows the relative permittivity (ε_r) of PTFE sheet as the function of temperature ranging from −20 to 150 °C as its test frequency is 120 Hz. b) The charging for a capacitor (50 V, 2 μF) with the load resistance R (510 Ω) at various temperatures within 300 s. The inset shows the Schematic circuit diagram of TENG for charging a capacitor through a full-bridge rectifier. c–f) Finite-element simulation about the space potential distribution of TENG and its color gradient bar with different potential values under different temperatures: c) −20 °C, d) 20 °C, e) 60 °C, and f) 150 °C. The up-plate is Al elctronde, the down-plate is PTFE sheet. The deeper red color (or blue color) is, the more positive (or negative) the space potential is.

contact electrification is given by Chowdry and Westgate,[36]

$$\sigma_P(x) = q^2 \bar{N}_t V(x) = q\bar{N}_t(\phi_{Al} - \phi_P)\exp(-\frac{x}{l_t}) \quad (1)$$

$$l_t = \left(\frac{\varepsilon}{q^2 \bar{N}_t}\right)^{1\backslash 2}$$

where, $V(x)$ is the electric potential on the PTFE sheet, l_t is the Debye length, q is the electron charge, the σ_p is the volume charge density of PTFE, $\bar{N}_t(/\mathrm{cm}^3 \cdot eV)$ is the volume defects density in unit energy. Here, the term defect is referred to those effective traps that can be occupied by electrons. The Φ_{Al} and Φp are the work function of the Al and PTFE, respectively. The chosen model, in this paper, is a simple and approximate model, that is, suitable for this paper to explain the effect of defect density and relative permittivity of PTFE on the charge density of PTFE surface.

Due to the principle of charge conservation, the same amount of positive charges will be induced on the Al electrode when two materials contact together. Therefore, we can calculate the electric surface density (σ_{Al}) on the Al electron,

$$\sigma_{Al} = -\int_0^{l_t} \sigma_p(x)dx = (\phi_P - \phi_{Al})(\varepsilon\bar{N}_t)^{1/2}\left(1 - \frac{1}{e}\right) \quad (2)$$

Then, the quantity of charges ΔQAl could be described by,

$$\Delta Q_{Al} = S\sigma_{Al} = S(\phi_P - \phi_{Al})(\varepsilon\bar{N}_t)^{1/2}\left(1 - \frac{1}{e}\right) \quad (3)$$

We assumed the electric charges on the Al electrode will transfer totally through external circuit to form short circuit current, so the amount of transferred charges (ΔQ_{sc}) can be described by

$$\Delta Q_{sc} = Q_{Al} = S(\phi_P - \phi_{Al})(\varepsilon\bar{N}_t)^{1/2}\left(1 - \frac{1}{e}\right) \quad (4)$$

To our best knowledge, the work function of Al and PTFE is 4.30 and 5.75 eV, respectively.[37] By quantitatively fitting the experimental data, we can obtain a nonlinear fitting equation of the relative permittivity of PTFE, as shown in Equation 5 and its numerical fitted curve is shown in Figure 4a.

$$\varepsilon_r = -5.86037 \times 10^{-8}T^3 + 8.38492 \times 10^{-6}T^2 - 7.02889 \times 10^{-4}T + 2.05 \quad (5)$$

The amount of transferred charges (ΔQ_{sc}) are influenced by the temperature-induced changes of relative permittivity and effective traps density $\bar{N}_t$ from the Equation 4. First of all, only the temperature effect on relative permittivity of PTFE was taken into regarded and the influence of effective traps density $\bar{N}_t$ on (ΔQ_{sc}) was ignored, we take $\bar{N}_t = 1.3 \times 10^{-5}/(cm^3 \cdot eV)$. Therefore, from Equations 4 and 5, the relationship between ΔQ_{sc} and T could be described by

$$\Delta Q_{sc} = 28.747 \times (-5.86037 \times 10^{-8}T^3 + 8.38492 \times 10^{-6}T^2 - 7.02889 \times 10^{-4}T + 2.05)^{\frac{1}{2}} \times 10^{-9}C \quad (6)$$

From Equation 6, the relation curve between the transferred charges and temperature can be achieved by taking $\bar{N}_t = 1.3 \times 10^{-5}/(cm^3 \cdot eV)$ shown in Figure 4b, which is basically accordant with the measurement of short-circuit transferred charges. The difference of theoretical calculation and experimental measurement of transferred charges may be the temperature-induced

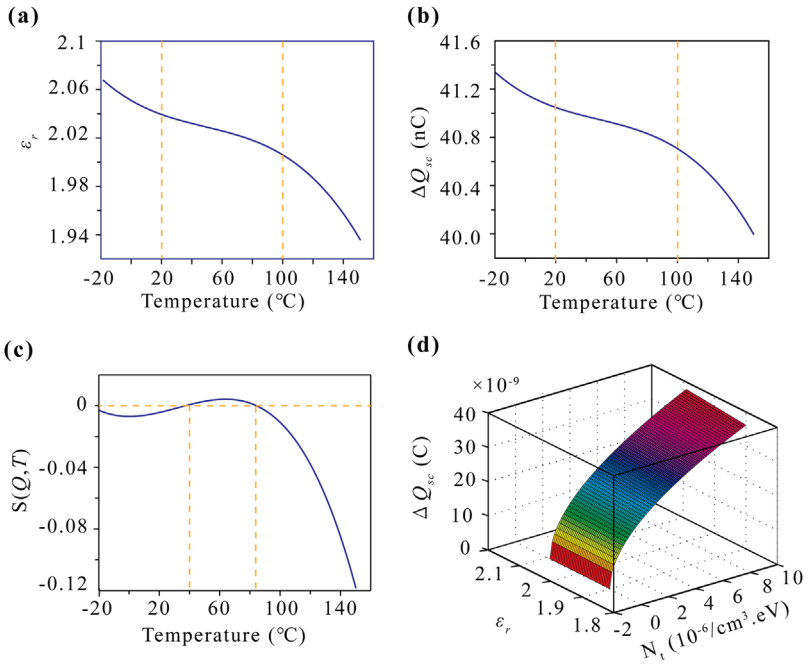

Figure 4. a) The curve of nonlinear fitting equation of the relative permittivity of PTFE sheet. b) The theoretical calculation of transferred charges of TENG at various temperature conditions ($N_t = 1.3 \times 10^{-5}/cm^3$ eV), only the temperature effect on relative permittivity of PTFE was taken into regarded. c) The coefficient sensitivity of ΔQ_{sc} to T, which is just contributed by the temperature indcued changes of relative permittivity of PTFE. d) The ΔQ_{sc} of TENG under the combined effect of ε_r and N_t.

changes of the number of effective traps. Therefore, $S(\Delta Q_{sc}, T)$, the sensitivity coefficient of ΔQ_{sc} to T, can be defined by using the ratio of relative change of both ΔQ_{sc} and T,

$$S(\Delta Qsc, T) = \frac{d\Delta Qsc}{dT} \times \frac{T}{\Delta Qsc}$$

$S(\Delta Q_{sc}, T) > 0$ means that the growing temperature will cause the increase in ΔQ_{sc}. In contrast, $S(\Delta Q_{sc}, T) < 0$ indicates that ΔQ_{sc} will be reduced as the temperature rises. For example, $S(\Delta Q_{sc}, T)$ is -0.1 when temperature is 140 °C, and it means that 1% increase in temperature will lead to 10% decrease of ΔQ_{sc}. There is a little increase of ΔQ_{sc} in the temperature range of 40–85 °C, but the ΔQ_{sc} drops rapidly when the temperature is above 90 °C or below 40 °C, shown in Figure 4c. It is accordant with the profile shown in Figure 2f.

In addition, the ΔQ_{sc} is also related to $\bar{N}_t$ according to Equation 3. The electrical output of TENG as a function of ε_r and $\bar{N}_t$ is shown in Figure 4d. It implies that the decrease of ε_r and $\bar{N}_t$ will weaken the PTFE's ability of bound electrons during the triboelectrification process. The triboelectric charges on the PTFE just are generated on the several hundred nanometers thin layer of the PTFE surface during a process of contact/friction electrification.[36] We suppose the effect of temperature perturbation would decline the stability of charges so that the magnitude of charges on the PTFE thin layer of surface would be reduced base on the theoretical calculations. And the more and more defects that can be occupied may be reduced owning to reduction of dangling bonds of the PTFE surface.

3.5. The Characterization of PTFE Sheets

The SEM images of PTFE sheet after the TENG worked at different conditions are shown in **Figure 5**. There are more and more flaking off thin sheets or small debris on the worn PTFE surface as the temperature rises. More and more flaking off thin sheets indicate that the intermolecular bonding force of PTFE become weaker even chemical bonds rupture. The abrasion resistance of PTFE get worse when the temperature rises.[38]

Secondly, the FTIR spectra of PTFE sheet after friction with the Al electrode at various temperatures is illustrated in **Figure 6**a. Figure 6b shows that the absorption bands appear at 773 and 793 cm^{-1} owing to the presence of group CF_2O.[39,40] As shown in Figure 6c, three absorption bands which reveal the asymmetric stretching vibration and stretching vibration of $-CF_2$ appear at about 1100–1300 cm^{-1} when the temperature is below 70 °C, but they gradually become a single wide absorption peak when the temperature increase from

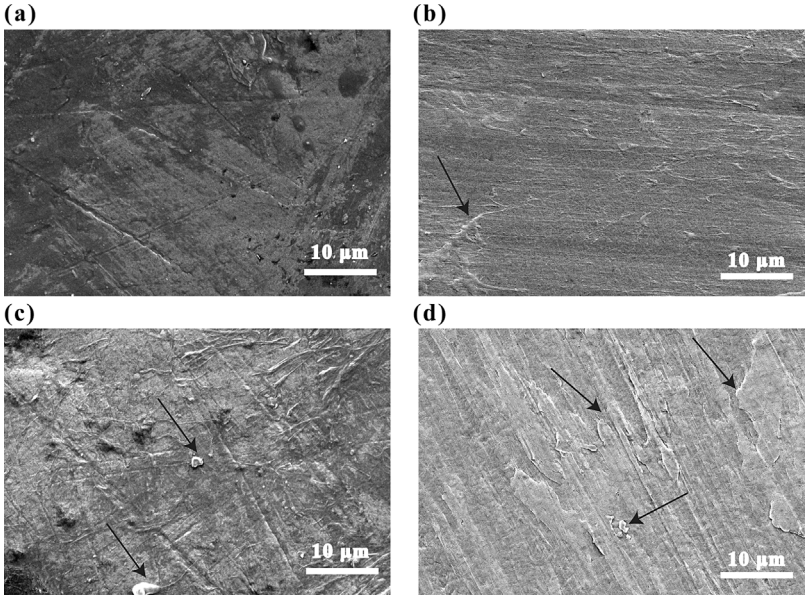

Figure 5. SEM photographs of the PTFE and flaking off thin sheets (as the pointing of arrows). a) is the photo of primitive PTFE without friction. And the PTFE after friction 10 min with Al electrode at different temperatures: b) −20 °C, c) 30 °C, d) 150 °C.

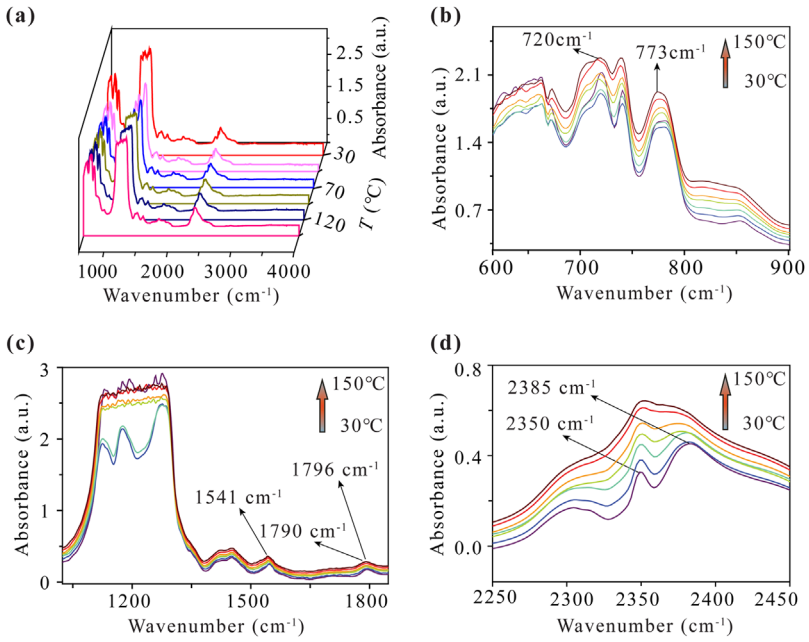

Figure 6. a) The FTIR absorption spectra of PTFE versus various temperatures (30, 50, 70, 90, 110, 130, and 150 °C, respectively). The absorbance peak from: b) 600 cm^{-1} to 900 cm^{-1}, c) 1050 cm^{-1} to 1800 cm^{-1}, d) 2250 cm^{-1} to 2450 cm^{-1}.

70 °C. This changes of the absorption peaks may be interpreted as the relaxation of PTFE crystal and the regular spiral chain of PTFE turning into irregular winding due to the effect of thermal perturbation. Figure 6d shows two absorption peaks appear at 2350 cm^{-1} (O═C═O) and 2383 cm^{-1}. But, the two absorption peaks gradually turn into a big single peak (nearby 2350 cm^{-1}). It indicates the PTFE surface would absorb more and more CO_2, when the temperature rises from 30 to 150 °C. The carbonyl group is observed at 1700–1800 cm^{-1} (C═O stretching), 720 cm^{-1} ($-CF_2$ scissoring).[41] The absorption peak at 1790 cm^{-1} has been identified as olefin end group $-CF{=}CF_2$[42] shown in Figure 6c.

As shown in previous research,[31] the above reactions analogous to those encountered in hydrocarbon oxidation that can occur on the effect of electric field in the air, such as

$$-CF_2 + O_2 \rightarrow -CF_2O_2\cdot \rightarrow -CF_2O\cdot$$
$$-CF_2CF_2CF_2 + O_2 \rightarrow -CF_2CF_2COF + F$$

The electron traps on the PTFE are mainly attributed to quantities of F atoms existing on the surface of PTFE due to its molecular chain with C atoms surrounded by F atoms spirally.[43] According to the IR absorption spectra of PTFE, we could know that the dangling bonds on the PTFE surface will react with the oxygen-containing electron acceptors in the air to form various oxygen-containing groups. This means that the oxygen atoms may occupy the positions of some fluorine atoms or combine with the dangling bonds of C atoms on the PTFE surface, which is a type of the electron traps. This is a process that temperature accelerate the surface oxidation and defluorinate on the PTFE surface, which may add the antistatic propensity of the polymers.[44,45] As the electron affinity of fluorine is stronger than oxygen, the molecular chains occupied by oxygen atoms would attract fewer electrons than the intact molecular chains. Besides, the molecular weight of PTFE would increase when the fluorine atoms are replaced largely by oxygen atoms. The increase of molecular weight will cause the decrease of relative permittivity of PTFE surface thin layer, according to the Clausius–Mossotti relation. For the reasons given above, the ability of PTFE about storing and gaining electrons will become weaker, so that result in the decreased electrical output of TENG along with the temperature rising.

Figure 7a and b, respectively, demonstrates the O 1 s and C 1 s peaks of PTFE characterized by XPS. As shows in Figure 7b, a shift of bonding energy can be evaluated to about 0.4 ± 0.2 eV for each oxygen atom and is roughly additive with the augment of temperature (C 1 s (2) at a binding energy E_b = 292.5 eV). The binding energy shift of C 1 s (2) is due to an inductive effect, which is dependent on the number of O atoms replaced position of F atoms and combined with dangling bonds of C atoms. As we know, the

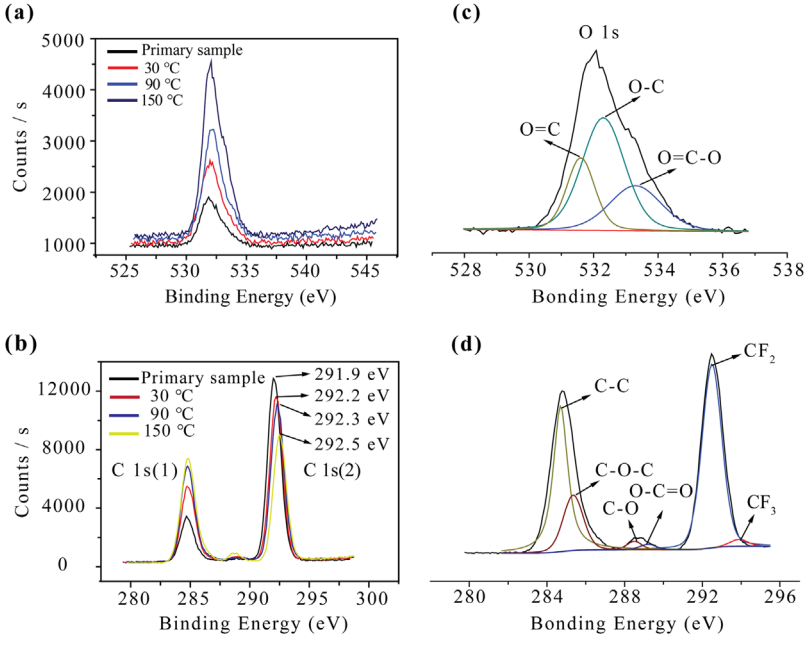

Figure 7. The XPS narrow scan spectra of four PTFE samples under different treatments: a) The O 1 s peak and b) the C 1 s peak under different conditions: the primary PTFE sample without contact or friction under 30, 90, and 150 °C. c) and d) demonstrate, respectively, the O and C peak fitting of XPS spectra of PTFE after a friction process under 150 °C environment.

Table 1. Surface elementary compositions of the PTFE sheets: Primary sample (without friction or contact), and the sample contacted with an Al electrode under 30, 90, and 150 °C.

	Elementary composition [%]			Atom ratio [%]	
Condition	C 1s	O 1s	F 1s	C/O	F/C
Primary sample	33.93	1.22	64.58	27.81	1.90
30 °C	37.54	2.20	59.89	17.06	1.60
90 °C	41.15	2.84	55.60	14.49	1.35
150 °C	41.7	4.63	53.37	9.01	1.30

magnitude of electronegativity ranks in following order: F>O>C. Owing to the difference of electronegativity between oxygen and fluorine, the ability of oxygen to attract electron is weaker than fluorine. Therefore, the PTFE attract less and less electrons during the friction process with the increase of temperature. Figure 7c and d show, respectively, the O and C peak fitting of XPS spectra of PTFE sheet contacted vertically with Al electrode at the temperature condition of 150 °C. The binding energy of C (1 s) in those chemical groups will be 284.6 eV (C—C), 292.5 eV (−(CF_2—CF_2)—n),[46,47] 286.45 eV (C—O—C),[46] 294.1 eV (−CF_3), 298.2 eV (O—C═O), and 288.5 eV (C—O).[41] **Table 1** (please see the Supporting Information for detail) describes the surface element compositions from the XPS data for PTFE sheets. The surface oxygen concentrations were in the range of 1.22–4.63%. The atom ratio of F/C reduces gradually, when the temperature rises during the friction process. This fact gives clear indication that the fluorine atoms are replaced by oxygen to form oxygen-containing chemical bonds. Namely, defluorination or surface oxidation is stronger with the increase of temperature. Thus, it means that more and more chemical groups occur on the surface of PTFE with the temperature growing. From the above analysis, the increase of oxygen-containing groups is possibly another factor that affects the electrical output performance of TENG.

4. Conclusion

In summary, the effected temperature performance of TENG was investigated experimentally and numerically in a variable temperature system. It is found that electrical output performance such as short-circuit current, open-circuit voltage, and short-circuit transferred charge of the TENG decrease with the augment of temperature from −20 to 20 °C. Although the short-circuit current and open-circuit voltage have trends of small increasing when the temperature changes from 20 to 60 °C and then decrease a little, they can be regarded as keeping stable in the whole temperature range of 20–100 °C, but drop rapidly when the temperature grows continuously. The variations in relative permittivity of PTFE, which means that its ability of storing charges show similar variation patterns to the electrical output of TENG. Based on the experiment and the theoretical analysis, the changes of relative permittivity and effective defects on the PTFE surface are contributed to this temperature-induced effect as the temperature increases. This work could provide meaningful information for the application of TENG in both power generation and self-powered sensing in the harsh environments.

Supporting Information

Supporting Information is available from the Wiley Online Library or from the author.

Acknowledgement

This research is supported by the "Thousands Talents" Program for Pioneer Researcher and His Innovation Team, China, the National Key R & D Project from Minister of Science and Technology (2016YFA0202704), National Natural Science Foundation of China (Grant No. 51432005, 5151101243, 51561145021, 61504009, and 51608039).

Conflict of Interest

The authors declare no conflict of interest.

Keywords

relative permittivity; surface electron traps; temperature effect; triboelectric nanogenerator

Received: March 27, 2017
Revised: May 26, 2017
Published online:

[1] N. S. Lewis, *Science* **2007**, *315*, 798.
[2] M. S. Dresselhaus, I. L. Thomas, *Nature* **2001**, *414*, 332.
[3] Z. L. Wang, W. Wu, *Angew. Chem.* **2012**, *51*, 11700.
[4] X. Chen, C. Li, M. Gratzel, R. Kostecki, S. S. Mao, *Chem. Soc. Rev.* **2012**, *41*, 7909.
[5] M. A. Fonseca, J. M. English, M. Von Arx, M. G. Allen, *J. Microelectromech. Syst.* **2002**, *11*, 337.
[6] E. Birdsell, M. G. Allen, *Solid-State Sens. Actuators Microsyst. Workshop* **2006**, *6*, 212.
[7] K. Takahata, Y. B. Gianchandani, *Sensors* **2008**, *8*, 2317.
[8] E. L. Tan, W. N. Ng, R. Shao, B. D. Pereles, K. G. Ong, *Sensors* **2007**, *7*, 1747.
[9] Z. Wang, L. Cheng, Y. Zheng, Y. Qin, Z. L. Wang, *Nano Energy* **2014**, *10*, 37.
[10] Y. Yu, G. Qiao, J. Ou, *IEEE Sens. J.* **2010**, *10*, **1901**.
[11] M. Han, X.-S. Zhang, X. Sun, B. Meng, W. Liu, H. Zhang, *Sci. Rep.* **2014**, *4*, 4811.
[12] M. Ha, J. Park, Y. Lee, H. Ko, *ACS Nano* **2015**, *9*, 3421.
[13] W. Tang, C. B. Han, C. Zhang, Z. L. Wang, *Nano Energy* **2014**, *9*, 121.
[14] J. H. Kim, J. Chun, J. W. Kim, W. J. Choi, J. M. Baik, *Adv. Funct. Mater.* **2015**, *25*, 7049.
[15] X. H. Li, C. B. Han, T. Jiang, C. Zhang, Z. L. Wang, *Nanotechnology* **2016**, *27*, 085401.
[16] P. Song, S. Kuang, N. Panwar, G. Yang, D. J. H. Tng, S. C. Tjin, W. J. Ng, M. B. A. Majid, G. Zhu, K. T. Yong, *Adv. Mater.* **2017**, *29*, 1605668.
[17] R. Hinchet, S.-W. Kim, *ACS Nano* **2015**, *9*, 7742.
[18] B. Saravanakumar, S. Soyoon, S.-J. Kim, *ACS Appl. Mater. Interfaces* **2014**, *6*, 13716.
[19] X. Wen, Y. Su, Y. Yang, H. Zhang, Z. L. Wang, *Nano Energy* **2014**, *4*, 150.
[20] Y. Su, J. Chen, Z. Wu, Y. Jiang, *Appl. Phys. Lett.* **2015**, *106*, 013114.
[21] C. A. Chang, Y. K. Kim, A. G. Schrott, *J. Vac. Sci. Technol. A: Vac. Surf. Films* **1990**, *8*, 3304.
[22] H. Unal, A. Mimaroglu, U. Kadıoglu, H. Ekiz, *Mater. Des.* **2004**, *25*, 239.
[23] S. K. Biswas, K. Vijayan, *Wear* **1992**, *158*, 193.
[24] D. W. Brown, L. A. Hymo, D. Michaelsen, *J. Res. Natl. Bur. Stand.* **1954**, *53*, 121.

[25] M. Li, C. Li, H. Zhan, J. Xu, X. Wang, *Appl. Phys. Lett*. **2008**, *92*, 1.
[26] S. Wang, Y. Xie, S. Niu, L. Lin, C. Liu, Y. S. Zhou, Z. L. Wang, *Adv. Mater*. **2014**, *26*, 6720.
[27] W. Yang, J. Chen, G. Zhu, J. Yang, P. Bai, Y. Su, Q. Jing, X. Cao, Z. L. Wang, *ACS Nano* **2013**, *7*, 11317.
[28] Z. Xu, L. Zhang, G. Chen, *J. Phys. D: Appl. Phys*. **2007**, *40*, 7085.
[29] T. A. D. L. Burgo, C. A. Rezende, S. Bertazzo, A. Galembeck, F. Galembeck, *J. Electrostat*. **2011**, *69*, 401.
[30] J. Krupka, K. Derzakowski, B. Riddle, J. Baker-Jarvis, *Meas. Sci. Technol*. **1999**, *9*, 1751.
[31] P. Ehrlich, *J. Res. Natl. Bur. Stand*. **1953**, *51*, 185.
[32] R. Elsdon, F. Mitchell, *J. Phys. D: Appl. Phys*. **1976**, *9*, 1445.
[33] C. B. Duke, T. J. Fabish, *J. Appl. Phys*. **1978**, *49*, 315.
[34] L.-H. Lee, *J. Electrostat*. **1994**, *32*, 1.
[35] J. Lowell, A. C. Rose-Innes, *Adv. Phys*. **2006**, *29*, 947.
[36] A. Chowdry, C. R. Westgate, *J. Phys. D: Appl. Phys*. **1974**, *7*, 713.
[37] S. Trigwell, N. Grable, C. U. Yurteri, R. Sharma, M. K. Mazumder, *IEEE Trans. Ind. Appl*. **2003**, *39*, 79.
[38] Y. Sujuan, Z. Xingrong, *Tribol. Trans*. **2014**, *57*, 382.
[39] J. H. Golden, *J. Polym. Sci*. **1960**, *XLV*, 534.
[40] P. J. H. Woltz, E. A. Jones, *J. Chem. Phys*. **1949**, *17*, 502.
[41] M. Nitschke, J. Meichsner, *J. Appl. Polym. Sci*. **1997**, *65*, 381.
[42] W. K. Fisher, J. C. Corelli, *J. Polym. Sci.: Polym. Chem. Ed*. **1981**, *19*, 2465.
[43] G. Zhang, K. Yang, W. Zhao, Z. Yan, *Appl. Surf. Sci*. **2006**, *253*, **1995**.
[44] E. Uchida, Y. Uyama, Y. Ikada, *Text. Res. J*. **1991**, *61*, 483.
[45] T. Onodera, K. Kawasaki, T. Nakakawaji, Y. Higuchi, N. Ozawa, K. Kurihara, M. Kubo, *J. Phys. Chem. C* **2014**, *118*, 5390.
[46] G. Nansé, E. Papirer, P. Fioux, F. Moguet, A. Tressaud, *Carbon* **1997**, *35*, 175.
[47] D. J. Wilson, A. J. Eccles, T. A. Steele, R. L. Williams, R. C. Pond, *Surf. Interface Anal*. **2000**, *30*, 36.